Task-Driven Lens Design: supplement

This document supplements the paper "Task-Driven Lens Design." It provides implementation details, validation of the optical simulation, additional results on multi-task performance (object detection and instance segmentation), comprehensive data for all designed lenses, and specifications of the realized designs.

1. IMPLEMENTATION DETAILS

Due to length constraints, the main paper (Sec. 4.1) provides only a brief overview of the implementation details. Here, we expand on those points and provide additional technical specifications. The design procedures vary slightly across different objectives and downstream tasks; we describe the specifics below.

A. Optical Lens

The optical lens comprises a sequence of aspherical surfaces. In our experiments, each surface profile is defined by:

$$z(r) = \frac{r^2}{R\left(1+\sqrt{1-(1+\kappa)\frac{r^2}{R^2}}\right)} + \alpha_4 r^4 + \alpha_6 r^6 + \alpha_8 r^8 + \alpha_{10} r^{10}, \tag{S1}$$

where $z(r)$ is the surface sag at radial distance $r = \sqrt{x^2+y^2}$, R is the radius of curvature, κ is the conic constant, and α_4 through α_{10} are the even-order aspheric coefficients. An additional parameter d denotes the thickness (or axial spacing) associated with each element. During the design process, we optimize the curvature $c = 1/R$, the thickness d, and the aspheric coefficients α_4 to α_{10}.

B. Point Spread Function

Optical rays originate from a point source in the object space and propagate through the refractive surfaces before intersecting the sensor plane. Given that our designs feature large apertures (low F-numbers) where geometric aberrations significantly outweigh diffraction effects, we employ a geometric PSF model. The intersection points on the sensor plane are binned into pixels to form the PSF. The PSF characterizes the impulse response of the optical system; the captured image is modeled as the convolution of the ideal image with this PSF. While an ideal, diffraction-free system would yield a Dirac delta PSF, real lenses exhibit blur due to optical aberrations. For RGB imaging, we compute PSFs at three primary wavelengths: 656.3 nm, 589.3 nm, and 486.1 nm.

C. Differentiable Ray Tracing

Our differentiable ray tracing engine is built upon the open-source DeepLens simulator [1] using PyTorch. During the forward pass, a computation graph is constructed to track gradients of ray-surface interactions and refraction. In the backward pass, gradients of the lens parameters are computed by differentiating through the ray-tracing operations via PyTorch's autograd engine. This end-to-end differentiability allows the lens parameters to be updated directly based on the gradients backpropagated from the downstream neural networks and task-specific loss functions.

D. Image Simulation

We utilize the ImageNet dataset [2] for both training and evaluation in the application of image classification. While commercial sensors typically offer megapixel resolution, standard training datasets are significantly smaller. Moreover, objects of interest rarely occupy the entire sensor field. To bridge this gap and accurately model field-dependent aberrations, we treat training images as localized patches centered at specific fields on the sensor. As illustrated in Fig. S1, we define nine point light sources in object space to sample the lens's field of view (FoV). Each input image is processed through all nine FoVs. The object distance is set to 20 m to approximate imaging at infinity. Given the short focal length and consequent short hyperfocal distance, optical properties remain stable beyond this depth; thus, we neglect depth-of-field effects, consistent with standard optical design practices. PSFs are first computed via ray tracing and then convolved with the input patches. Finally, a simple image signal processing (ISP) pipeline, which includes

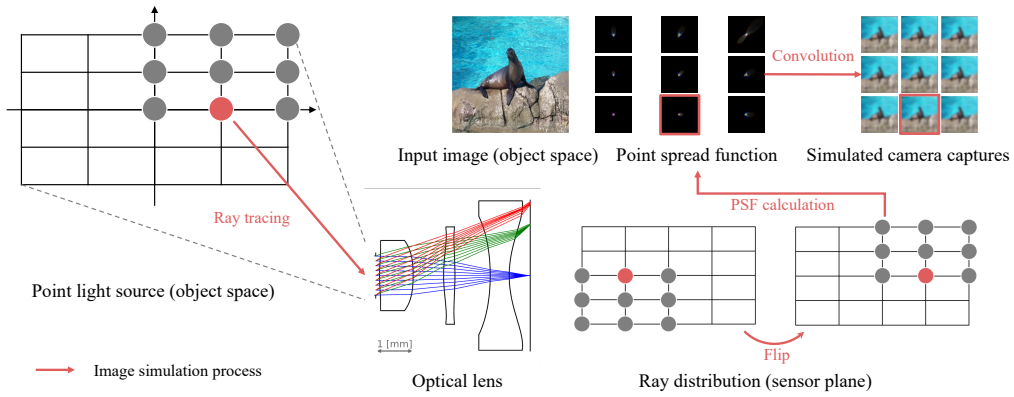

Fig. S1. Overview of the image simulation process. We first perform ray tracing to compute the Point Spread Function (PSF) at various fields of view (FoV). We then convolve the latent input image with these PSFs to simulate the sensor capture at each field location. To account for the high resolution of commercial sensors relative to standard training datasets, we model training images as patches corresponding to distinct field positions on the full sensor.

demosaicing, auto white balancing, and gamma correction, is applied to synthesize realistic sensor measurements.

E. Datasets

For **image classification**, ImageNet comprises 1,281,167 training images and 50,000 validation images. We report top-1 accuracy on the validation set. With the augmentation of nine FoVs per image, the effective dataset size increases to approximately 11.5 million training samples and 450,000 evaluation samples. We use a batch size of 64, which results in processing 576 simulated patches per iteration (64 images $\times$ 9 FoVs).

For **object detection**, we use the COCO 2017 dataset [3]. We train on the `train2017` split (118,287 images) and evaluate on `val2017` (5,000 images). Performance is measured using mean Average Precision (mAP) averaged over IoU thresholds from 0.50 to 0.95.

For **semantic segmentation**, we also employ COCO 2017 with segmentation annotations, utilizing the same splits as detection and reporting mAP according to the standard COCO protocol.

For **image–text retrieval**, we utilize the Flickr30k dataset [4], consisting of 31,783 images, each paired with five descriptive captions. We adhere to the standard split: 29,783 for training, 1,000 for validation, and 1,000 for testing, reporting Recall@1.

F. Data Augmentation

We apply data augmentation [5] to the training images, incorporating controlled degradations such as blur, noise, and color jitter. Augmentation is of great importance for task-driven lens design because it prevents the optimization from converging to specific aberration patterns (or a "perfect" but brittle optical state) and enhances the robustness of the designed lens to defocus and manufacturing tolerances.

G. TaskLens Design

For task-driven image classification, we employ a pre-trained ResNet-50 [6] as the backbone (via `timm`). The lens parameters are initialized randomly and optimized from scratch using the cross-entropy loss. The initial learning rates are detailed in Table S1. To ensure physical realizability and ray stability, we include a regularization term penalizing ray obliquity [1]. The total loss function is:

$$\mathcal{L} = \mathcal{L}_{\text{cls}}\big(f(g_\theta(x)), y\big) + \lambda\, \mathcal{L}_{\text{reg}}\,, \tag{S2}$$

where x is the input image, g_θ represents the optical simulation parameterized by lens variables θ, f is the classification network, and $\lambda = 0.1$ is the regularization weight. $\mathcal{L}_{\text{cls}}$ denotes the classification loss, while $\mathcal{L}_{\text{reg}}$ promotes smooth ray paths to prevent degenerate lens geometries.

Table S1. Learning rates for different lens parameters.

Curvature c	Position d	Polynomial α_4	Polynomial α_6	Polynomial α_8	Polynomial α_{10}
$1e^{-4}$	$1e^{-4}$	$1e^{-4}$	$2e^{-6}$	$4e^{-8}$	$8e^{-10}$

For other downstream tasks (object detection, semantic segmentation, and retrieval), we maintain the same optical design settings and learning rates, substituting the classification loss with the appropriate task-specific objective.

H. ImagingLens Design

For each TaskLens configuration, we design three baseline "ImagingLenses" optimized solely for image quality. **ImagingLens #1** is designed to minimize the Root Mean Square (RMS) spot radius across an 11×11 grid of fields, with 1024 rays traced per field. We employ curriculum learning [1] to optimize this lens from scratch within our differentiable framework, using the same hyperparameters and regularization as TaskLens. The remaining two baselines are optimized using **Zemax OpticStudio**. We start from a blank slate and use the standard merit function (RMS spot radius, referenced to centroid) with a Gaussian Quadrature sampling (16 rings, 12 arms). Constraints are applied to ensure positive element thicknesses. The entrance pupil diameter is fixed, while the effective focal length (and thus F-number) is allowed to vary to satisfy first-order properties. All radii, aspheric coefficients, and thicknesses are set as variables.

2. ADDITIONAL RESULTS

We render images from the COCO 2017 validation set with our optical simulator using the three-element TaskLens and the corresponding ImagingLens (triplet #1). For object detection, we use the official pretrained "faster_rcnn_R_50_FPN_3x" model from Detectron2 without lens-specific fine-tuning. For segmentation, we show panoptic segmentation using the Mask2Former model with a Swin-Small backbone from HuggingFace, also without fine-tuning. Across representative examples, the TaskLens yields more correct and higher-confidence detections and produces cleaner panoptic segmentations with fewer artifacts and more consistent region boundaries than the ImagingLens.

Fig. S2. Qualitative object detection results. Left: TaskLens (triplet). Right: ImagingLens (triplet #1). We use the official pretrained "faster_rcnn_R_50_FPN_3x" model without fine-tuning for each lens. Left example: more people are detected in the TaskLens simulated image. Right example: the traffic light is successfully detected only in the TaskLens simulated image (marked by the red box). Moreover, detection boxes in the TaskLens render images usually have higher confidence.

3. ADDITIONAL DATA

A. Lens Data

Figure S4 shows all designed ImagingLenses and the image classification TaskLens. We also provide the detailed lens data in Table S2 to Table S16. The data format is similar to the Zemax lens data format, which we think is easy to understand. The "Thickness" term represents the distance to the next surface. "End2EndLens" represents the End-to-End training results from the best ImagingLens.

Table S2. Lens data for the 2P TaskLens.

Surface	Thickness [mm]	Curvature $[mm]^{-1}$	Diameter [mm]	Material	α_4	α_6	α_8	α_{10}
1 (Aper)	0.100		1.04					
2 (Asphere)	1.108	0.2279	1.32	OKP4	-6.230556e-02	-2.692730e-03	2.011200e-04	4.264318e-06
3 (Asphere)	0.869	-0.1988	1.96	AIR	-3.943852e-02	6.418004e-03	6.530462e-04	1.290069e-05
4 (Asphere)	0.847	0.2406	2.69	PMMA	-5.051126e-02	-6.483181e-03	-2.742670e-04	-6.921774e-06
5 (Asphere)	1.463	-0.0379	3.17	AIR	3.602685e-03	-4.919978e-03	-4.744795e-05	4.207488e-06
6 (Sensor)			4.00					

Table S3. Lens data for the 2P ImagingLens #1.

Surface	Thickness [mm]	Curvature $[mm]^{-1}$	Diameter [mm]	Material	α_4	α_6	α_8	α_{10}
1 (Aper)	0.100		1.04					
2 (Asphere)	1.110	0.2093	1.55	OKP4	-3.557858e-02	-2.151537e-03	2.138008e-04	4.856510e-06
3 (Asphere)	0.858	-0.1934	2.19	AIR	-5.836600e-02	5.725940e-03	5.713565e-04	7.521212e-06
4 (Asphere)	0.855	0.2525	2.86	PMMA	-5.963345e-02	-6.859528e-03	-2.956688e-04	-8.457044e-06
5 (Asphere)	1.514	-0.0675	3.30	AIR	6.357471e-03	-4.605474e-03	-2.022348e-05	6.599236e-06
6 (Sensor)			4.00					

Table S4. Lens data for the 2P ImagingLens #2.

Surface	Thickness [mm]	Curvature $[mm]^{-1}$	Diameter [mm]	Material	α_4	α_6	α_8	α_{10}	α_{12}
1 (Aper)	0.100		1.04						
2 (Asphere)	0.828	0.2632	1.10	OKP4	-2.941442e-02	-1.739322e-02	-5.028618e-02	1.460911e-02	7.344432e-01
3 (Asphere)	1.160	-0.1006	1.80	AIR	-7.069314e-02	4.010654e-03	-6.927734e-03	3.027622e-04	9.092269e-03
4 (Asphere)	1.303	0.4436	2.54	PMMA	-5.967423e-02	-8.591303e-03	-4.543824e-03	-9.672559e-04	-1.942622e-03
5 (Asphere)	1.082	0.1736	3.42	AIR	1.812585e-02	-1.161345e-02	-1.200210e-03	-4.974294e-05	-5.326503e-06
6 (Sensor)			3.90						

Table S5. Lens data for the 2P ImagingLens #3.

Surface	Thickness [mm]	Curvature $[mm]^{-1}$	Diameter [mm]	Material	α_4	α_6	α_8	α_{10}	α_{12}
1 (Aper)	0.100		1.04	AIR					
2 (Asphere)	1.190	0.2718	1.27	OKP4	-3.195822e-02	-2.216966e-02	-5.040844e-02	1.460761e-02	7.344432e-01
3 (Asphere)	0.812	-0.0909	1.92	AIR	-6.991725e-02	3.324919e-03	-6.962574e-03	3.018416e-04	9.092269e-03
4 (Asphere)	1.247	0.4497	2.60	PMMA	-5.536971e-02	-7.750550e-03	-4.525531e-03	-9.670507e-04	-1.942622e-03
5 (Asphere)	1.124	0.1734	3.49	AIR	2.866083e-02	-1.051536e-02	-1.155842e-03	-4.851578e-05	-5.297208e-06
6 (Sensor)			4.00	AIR					

Table S6. Lens data for the 2P End2EndLens.

Surface	Thickness [mm]	Curvature $[mm]^{-1}$	Diameter [mm]	Material	α_4	α_6	α_8	α_{10}	α_{12}
1 (Aper)	0.100		1.04	AIR					
2 (Asphere)	1.111	0.2665	1.33	OKP4	-3.540349e-02	-1.654536e-02	-5.024989e-02	1.460925e-02	7.344432e-01
3 (Asphere)	0.837	-0.0989	1.93	AIR	-7.081930e-02	3.693011e-03	-6.945701e-03	3.021957e-04	9.092269e-03
4 (Asphere)	1.348	0.4429	2.60	PMMA	-7.077941e-02	-8.365979e-03	-4.539080e-03	-9.672103e-04	-1.942622e-03
5 (Asphere)	1.076	0.2188	3.60	AIR	1.354988e-02	-1.232918e-02	-1.213283e-03	-4.982987e-05	-5.323246e-06
6 (Sensor)			3.90	AIR					

Table S7. Lens data for the 3P TaskLens.

Surface	Thickness [mm]	Curvature $[mm]^{-1}$	Diameter [mm]	Material	α_4	α_6	α_8	α_{10}
1 (Aper)	0.100			AIR				
2 (Asphere)	0.887	0.2405	1.32	PMMA	-1.201920e-01	-7.420412e-03	4.264761e-05	3.585087e-07
3 (Asphere)	0.804	-0.2585	1.86	AIR	-1.485584e-01	-3.720956e-03	4.013637e-04	8.193966e-06
4 (Asphere)	0.299	0.2408	2.49	OKP4	-4.984390e-02	-2.352248e-03	-1.390607e-04	-4.099868e-06
5 (Asphere)	0.930	-0.1243	2.58	AIR	3.638798e-02	-1.723573e-03	-1.122244e-04	3.827879e-07
6 (Asphere)	0.501	-0.1916	3.14	PMMA	-9.229322e-03	-1.210485e-05	-1.093474e-04	-3.512698e-06
7 (Asphere)	0.554	0.3484	3.96	AIR	-1.864598e-02	-2.933642e-03	-1.108433e-04	6.989184e-07
8 (Sensor)			4.00	AIR				

Fig. S3. Panoptic segmentation results. Left: TaskLens (triplet). Right: ImagingLens (triplet #1). We use Mask2Former (Swin-Small backbone) without fine-tuning for each lens. Segmentation results on TaskLens rendered images contain fewer artifacts. The corresponding detection results have higher confidence.

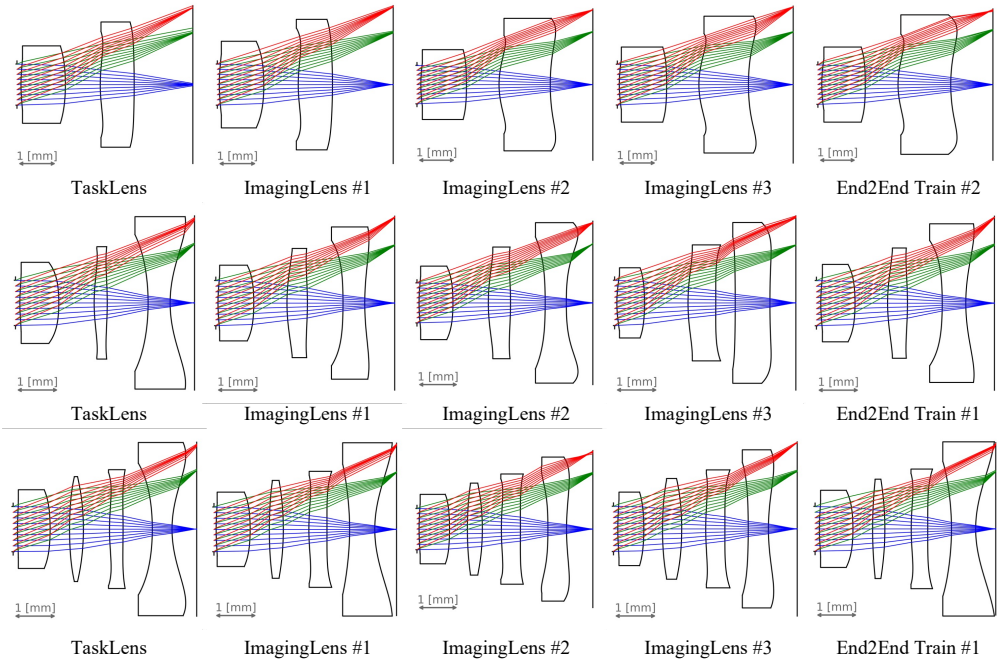

Fig. S4. All designed ImagingLenses and the image classification network.

B. Actual Lens Specifications

Achieving uniform field of view (FoV) and effective imaging height across different lens designs is challenging. To ensure the TaskLens is not achieving better task results by adopting less challenging specifications, we analyze the optical specifications for each lens in Table S17. Generally, for a fixed number of elements, a wider FoV requires stronger ray bending and tighter aberration control over the image field, which makes the optical design more challenging. Likewise, accommodating a larger sensor diagonal increases the required image circle and vignetting control, which is also more challenging. In Table S17, TaskLens pairs wide FoV (about 69.5°–70.7°) with the target 4.0 mm sensor diagonal across 2P/3P/4P configurations, whereas some imaging baselines that report a slightly wider FoV do so while using a smaller sensor diagonal (3.8–3.9 mm). This indicates that TaskLens is not benefiting from less demanding specifications.

REFERENCES

1. X. Yang, Q. Fu, and W. Heidrich, "Curriculum learning for ab initio deep learned refractive optics," Nat. Commun. **15**, 50835 (2024).
2. J. Deng, W. Dong, R. Socher, *et al.*, "ImageNet: A large-scale hierarchical image database," in *CVPR*, (Ieee, 2009), pp. 248–255.
3. T.-Y. Lin, M. Maire, S. Belongie, *et al.*, "Microsoft coco: Common objects in context," in

Table S8. Lens data for the 3P ImagingLens #1.

Surface	Thickness [mm]	Curvature $[mm]^{-1}$	Diameter [mm]	Material	α_4	α_6	α_8	α_{10}
1 (Aper)	0.100		1.04	AIR				
2 (Asphere)	0.814	0.2476	1.25	PMMA	-7.998895e-02	-4.237434e-03	1.447068e-04	2.772055e-06
3 (Asphere)	0.756	-0.2059	1.74	AIR	-1.213981e-01	-9.009774e-04	4.764367e-04	9.609429e-06
4 (Asphere)	0.465	0.2307	2.41	OKP4	-2.160468e-02	-2.337896e-03	-1.632334e-04	-4.971110e-06
5 (Asphere)	0.811	-0.1190	2.51	AIR	3.271303e-02	-9.073227e-04	-7.741294e-05	1.429375e-06
6 (Asphere)	0.495	-0.0881	2.88	PMMA	-3.529020e-02	-1.742304e-03	-1.535450e-04	-4.782808e-06
7 (Asphere)	0.683	0.1661	3.50	AIR	-1.497258e-02	-1.607410e-03	-6.544410e-05	2.114299e-06
8 (Sensor)			4.00	AIR				

Table S9. Lens data for the 3P ImagingLens #2.

Surface	Thickness [mm]	Curvature $[mm]^{-1}$	Diameter [mm]	Material	α_4	α_6	α_8	α_{10}
1 (Aper)	0.100		1.04	AIR				
2 (Asphere)	0.804	0.2249	1.27	PMMA	-5.094405e-02	-6.908586e-03	1.420362e-04	1.420362e-04
3 (Asphere)	0.839	-0.2117	1.76	AIR	-1.059854e-01	-4.538634e-03	5.032599e-04	5.032599e-04
4 (Asphere)	0.527	0.2259	2.52	OKP4	-2.178941e-02	-4.585173e-03	-1.803447e-04	-1.803447e-04
5 (Asphere)	0.822	-0.1137	2.67	AIR	2.632563e-02	1.512580e-03	-6.432167e-05	-6.432167e-05
6 (Asphere)	0.501	-0.0733	3.16	PMMA	-3.297533e-02	5.560323e-03	-1.589946e-04	-1.589946e-04
7 (Asphere)	0.629	0.1155	3.84	AIR	6.755690e-02	-1.823045e-02	-6.960762e-05	-6.960762e-05
8 (Sensor)			3.91	AIR				

Computer vision–ECCV 2014: 13th European conference, zurich, Switzerland, September 6-12, 2014, proceedings, part v 13, (Springer, 2014), pp. 740–755.

4. P. Young, A. Lai, M. Hodosh, and J. Hockenmaier, "From image descriptions to visual denotations: New similarity metrics for semantic inference over event descriptions," Trans. association for computational linguistics **2**, 67–78 (2014).
5. S. G. Müller and F. Hutter, "TrivialAugment: Tuning-free yet state-of-the-art data augmentation," in *ICCV,* (2021), pp. 774–782.
6. K. He, X. Zhang, S. Ren, and J. Sun, "Deep residual learning for image recognition," in *CVPR,* (2016), pp. 770–778.

Table S10. Lens data for the 3P ImagingLens #3.

Surface	Thickness [mm]	Curvature $[mm]^{-1}$	Diameter [mm]	Material	α_4	α_6	α_8	α_{10}
1 (Aper)	0.100		1.04	AIR				
2 (Asphere)	0.629	0.3452	1.28	PMMA	-7.871836e-02	-5.350309e-03	2.320887e-04	1.445756e-04
3 (Asphere)	0.990	-0.1742	1.61	AIR	-9.910008e-02	-1.127885e-02	3.269837e-04	4.994923e-04
4 (Asphere)	0.633	0.2240	2.42	OKP4	-2.066278e-02	-7.454170e-03	-2.438883e-04	-1.814870e-04
5 (Asphere)	0.442	-0.0203	2.66	AIR	3.662718e-02	1.895413e-03	2.899968e-05	-5.955982e-06
6 (Asphere)	0.790	-0.0176	3.05	PMMA	-3.742982e-03	2.071768e-04	-2.769423e-04	-1.612489e-04
7 (Asphere)	0.591	0.0352	3.69	AIR	1.604678e-02	-1.050925e-02	9.399757e-05	-6.632384e-05
8 (Sensor)			4.00	AIR				

Table S11. Lens data for the 3P End2EndLens.

Surface	Thickness [mm]	Curvature $[mm]^{-1}$	Diameter [mm]	Material	α_4	α_6	α_8	α_{10}
1 (Aper)	0.100		1.04	AIR				
2 (Asphere)	0.783	0.2446	1.32	PMMA	-7.827187e-02	-3.493498e-03	1.676159e-04	3.248085e-06
3 (Asphere)	0.745	-0.2121	1.78	AIR	-1.202044e-01	-1.351351e-03	4.594656e-04	9.180380e-06
4 (Asphere)	0.455	0.2390	2.42	OKP4	-2.908486e-02	-2.039731e-03	-1.408897e-04	-4.239835e-06
5 (Asphere)	0.795	-0.1285	2.53	AIR	3.206206e-02	-1.436517e-03	-1.019131e-04	6.927270e-07
6 (Asphere)	0.539	-0.1120	2.88	PMMA	-3.670126e-02	-1.170376e-03	-1.327894e-04	-4.211608e-06
7 (Asphere)	0.656	0.2392	3.65	AIR	-1.337205e-02	-2.322827e-03	-8.910213e-05	1.504667e-06
8 (Sensor)			4.00	AIR				

Table S12. Lens data for the 4P TaskLens.

Surface	Thickness [mm]	Curvature $[mm]^{-1}$	Diameter [mm]	Material	α_4	α_6	α_8	α_{10}
1 (Aper)	0.100		1.04	AIR				
2 (Asphere)	0.742	0.1673	1.31	PMMA	-9.882198e-02	-5.059574e-03	1.236521e-04	2.401968e-06
3 (Asphere)	0.443	-0.1912	1.81	AIR	-8.171525e-02	-2.236586e-03	4.394940e-04	9.022501e-06
4 (Asphere)	0.315	0.1119	2.37	OKP4	1.488245e-02	-1.473840e-03	2.082270e-04	4.016732e-06
5 (Asphere)	0.595	-0.1655	2.41	AIR	-9.517191e-03	1.925957e-03	5.143318e-04	1.002425e-05
6 (Asphere)	0.308	0.1844	2.60	OKP4	-5.583153e-02	-3.878689e-03	-1.800252e-04	-4.731216e-06
7 (Asphere)	0.666	-0.0452	2.73	AIR	2.723789e-02	-6.684430e-04	-8.248209e-05	8.828483e-07
8 (Asphere)	0.448	-0.1958	3.03	PMMA	-1.434444e-02	-7.493469e-04	-1.249907e-04	-3.923112e-06
9 (Asphere)	0.564	0.3755	3.98	AIR	-2.438926e-02	-3.631569e-03	-1.352864e-04	2.475713e-07
10 (Sensor)			4.00	AIR				

Table S13. Lens data for the 4P ImagingLens #1.

Surface	Thickness [mm]	Curvature $[mm]^{-1}$	Diameter [mm]	Material	α_4	α_6	α_8	α_{10}
1 (Aper)	0.100		1.04	AIR				
2 (Asphere)	0.742	0.1673	1.31	PMMA	-9.882198e-02	-5.059574e-03	1.236521e-04	2.401968e-06
3 (Asphere)	0.443	-0.1912	1.81	AIR	-8.171525e-02	-2.236586e-03	4.394940e-04	9.022501e-06
4 (Asphere)	0.315	0.1119	2.37	OKP4	1.488245e-02	-1.473840e-03	2.082270e-04	4.016732e-06
5 (Asphere)	0.595	-0.1655	2.41	AIR	-9.517191e-03	1.925957e-03	5.143318e-04	1.002425e-05
6 (Asphere)	0.308	0.1844	2.60	OKP4	-5.583153e-02	-3.878689e-03	-1.800252e-04	-4.731216e-06
7 (Asphere)	0.666	-0.0452	2.73	AIR	2.723789e-02	-6.684430e-04	-8.248209e-05	8.828483e-07
8 (Asphere)	0.448	-0.1958	3.03	PMMA	-1.434444e-02	-7.493469e-04	-1.249907e-04	-3.923112e-06
9 (Asphere)	0.564	0.3755	3.98	AIR	-2.438926e-02	-3.631569e-03	-1.352864e-04	2.475713e-07
10 (Sensor)			4.00	AIR				

Table S14. Lens data for the 4P ImagingLens #2.

Surface	Thickness [mm]	Curvature $[mm]^{-1}$	Diameter [mm]	Material	α_4	α_6	α_8	α_{10}
1 (Aper)	0.100		1.04	AIR				
2 (Asphere)	0.778	0.1983	1.24	PMMA	-8.836898e-02	-4.262349e-03	1.490898e-04	3.101509e-06
3 (Asphere)	0.439	-0.2125	1.73	AIR	-9.584536e-02	-3.297418e-03	3.935776e-04	7.663079e-06
4 (Asphere)	0.320	0.0947	2.21	OKP4	7.747480e-03	-1.332338e-03	2.316622e-04	4.985073e-06
5 (Asphere)	0.585	-0.1425	2.27	AIR	-6.778305e-03	1.922866e-03	5.005212e-04	9.308818e-06
6 (Asphere)	0.414	0.1844	2.51	OKP4	-4.904995e-02	-4.319484e-03	-1.946336e-04	-4.974748e-06
7 (Asphere)	0.518	-0.0156	2.69	AIR	3.748472e-02	-1.111389e-05	-6.598805e-05	1.124154e-06
8 (Asphere)	0.575	-0.1522	3.02	PMMA	7.492220e-03	-1.415259e-03	-1.507766e-04	-4.519364e-06
9 (Asphere)	0.500	0.3507	4.00	AIR	-2.200943e-02	-8.533297e-04	-5.919880e-05	1.949792e-06
10 (Sensor)			3.80	AIR				

Table S15. Lens data for the 4P ImagingLens #3.

Surface	Thickness [mm]	Curvature $[\text{mm}]^{-1}$	Diameter [mm]	Material	α_4	α_6	α_8	α_{10}
1 (Aper)	0.100		1.04	AIR				
2 (Asphere)	0.592	0.1764	1.31	PMMA	-6.478445e-02	-3.352266e-03	1.649022e-04	3.217212e-06
3 (Asphere)	0.426	-0.1740	1.69	AIR	-6.794760e-02	-2.302133e-04	4.845259e-04	9.795038e-06
4 (Asphere)	0.437	0.1230	2.22	OKP4	1.165871e-02	-2.376378e-03	1.686029e-04	3.062514e-06
5 (Asphere)	0.547	-0.1491	2.31	AIR	-1.377027e-02	2.317677e-03	5.479770e-04	1.098924e-05
6 (Asphere)	0.436	0.1478	2.55	OKP4	-3.458765e-02	-3.592606e-03	-1.968449e-04	-5.557803e-06
7 (Asphere)	0.531	-0.0095	2.71	AIR	3.698580e-02	-4.438855e-05	-5.078399e-05	1.950553e-06
8 (Asphere)	0.460	-0.0474	3.05	PMMA	-1.109705e-02	-1.052585e-03	-1.413057e-04	-4.595032e-06
9 (Asphere)	0.654	0.1982	3.63	AIR	-1.286063e-02	-3.620622e-03	-1.336623e-04	5.103128e-07
10 (Sensor)			4.00	AIR				

Table S16. Lens data for the 4P End2EndLens.

Surface	Thickness [mm]	Curvature $[\text{mm}]^{-1}$	Diameter [mm]	Material	α_4	α_6	α_8	α_{10}
1 (Aper)	0.100		1.04	AIR				
2 (Asphere)	0.776	0.2094	1.31	PMMA	-9.001061e-02	-4.458418e-03	1.466841e-04	3.094893e-06
3 (Asphere)	0.455	-0.2221	1.79	AIR	-1.007577e-01	-3.324089e-03	3.923575e-04	7.613106e-06
4 (Asphere)	0.455	0.0908	2.25	OKP4	1.579886e-03	-1.668447e-03	2.300933e-04	5.049782e-06
5 (Asphere)	0.610	-0.1367	2.30	AIR	-4.271065e-03	2.299120e-03	5.036045e-04	9.268433e-06
6 (Asphere)	0.382	0.1769	2.58	OKP4	-4.762138e-02	-4.734586e-03	-2.010100e-04	-4.986154e-06
7 (Asphere)	0.549	-0.0095	2.77	AIR	3.225713e-02	4.351055e-05	-6.839795e-05	9.540291e-07
8 (Asphere)	0.559	-0.1621	3.12	PMMA	5.123787e-03	-1.587822e-03	-1.526139e-04	-4.454318e-06
9 (Asphere)	0.466	0.3675	4.04	AIR	-2.638335e-02	-2.740633e-04	-3.539184e-05	2.557922e-06
10 (Sensor)			4.00	AIR				

Table S17. Optical specifications for each lens. Among lenses with the same number of elements, TaskLens does not achieve better task results by adopting less challenging specifications.

		FoV	Sensor Diag [mm]
2P	TaskLens	69.5° (↑ 0.7%)	4.0
	ImagingLens #1	69.1° (↑ 0.4%)	4.0
	ImagingLens #2	70.6° (↑ 2.6%)	3.9 (↓ 2.5%)
	ImagingLens #3	69.5° (↑ 1.0%)	4.0
3P	TaskLens	70.7° (↑ 2.8%)	4.0
	ImagingLens #1	69.2° (↑ 0.6%)	4.0
	ImagingLens #2	69.1° (↑ 0.4%)	3.9 (↓ 2.5%)
	ImagingLens #3	69.1° (↑ 0.4%)	4.0
4P	TaskLens	70.0° (↑ 1.7%)	4.0
	ImagingLens #1	68.7° (↓ 0.2%)	4.0
	ImagingLens #2	70.6° (↑ 2.6%)	3.8 (↓ 5.0%)
	ImagingLens #3	69.3° (↑ 0.7%)	4.0